

$K(p, \pm 1; p, 0)$

$$= \frac{2V}{\pi} \frac{32}{15(a_1 a_2)^{5/2}} \left( \frac{a_1 a_2}{a_1 + a_2} \right)^7 \times \int_0^\infty \frac{k^6}{k^2 + \mu^2} e^{-k^2(a_1 a_2)/(a_1 + a_2)} dk, \quad (\text{A11})$$

$$K(p, \pm 1; p, \mp 1) = 2K(p, \pm 1; p, 0). \quad (\text{A12})$$

Similar, but more complicated results are obtained with the  $1p$  wave function given in Eq. (7).

The basic integral which was encountered,

$$\int_0^\infty \frac{k^2}{k^2 + \mu^2} e^{-k^2 a^2} dk, \quad (\text{A13})$$

was readily evaluated numerically. The other integrals which were needed were then calculated using the recurrence relation

$$\int_0^\infty \frac{k^{2n+2}}{k^2 + \mu^2} e^{-k^2 a^2} dk = \frac{\pi^{1/2} (2n-1)!!}{2^{n+1} \alpha^{2n+1}} \mu^2 \int_0^\infty \frac{k^{2n}}{k^2 + \mu^2} e^{-k^2 a^2} dk. \quad (\text{A14})$$

## Interactions of $^3\text{He}$ Particles with $^9\text{Be}$ , $^{12}\text{C}$ , $^{16}\text{O}$ , and $^{19}\text{F}^\dagger$

R. L. HAHN AND E. RICCI

Oak Ridge National Laboratory, Oak Ridge, Tennessee

(Received 27 January 1966)

Excitation functions for reactions induced by  $^3\text{He}$  particles in Be, C, O, and F were determined by irradiating thin foils of beryllium, Mylar, Teflon, and nylon with  $^3\text{He}$  ions of energies from 3 to 10 MeV. The radioactive products were assayed by gamma spectrometry, and their decay curves fitted by least-squares analysis. The maximum cross sections (and corresponding  $^3\text{He}$  energies) were  $^9\text{Be}(^3\text{He},n)^{11}\text{C}$ ,  $113 \pm 11$  mb (4.3 MeV);  $^{12}\text{C}(^3\text{He},n)^{14}\text{O}$ ,  $16.5 \pm 1.8$  mb (6.3 MeV);  $^{12}\text{C}(^3\text{He},d)^{13}\text{N}$ ,  $98.9 \pm 12.2$  mb (9.5 MeV);  $^{12}\text{C}(^3\text{He},\alpha)^{11}\text{C}$ ,  $366 \pm 26$  mb (8.2 MeV);  $^{16}\text{O}(^3\text{He},p)^{18}\text{F}$ ,  $436 \pm 44$  mb (6.3 MeV);  $^{16}\text{O}(^3\text{He},\alpha)^{14}\text{O}$ ,  $169 \pm 17$  mb (6.6 MeV);  $^{19}\text{F}(^3\text{He},\alpha)^{18}\text{F}$ ,  $22.1 \pm 2.0$  mb (7.1 MeV); and  $^{19}\text{F}(^3\text{He},\alpha)^{17}\text{F}$ ,  $50.4 \pm 5.0$  mb (8.2 MeV). Results for some of these reactions, previously obtained by other workers, were in reasonable agreement with our data; in particular, the fine structure of the reaction  $^{12}\text{C}(^3\text{He},n)^{14}\text{O}$  was confirmed in these experiments. An integral excitation function, calculated from the differential data of Towle and Macefield for the  $^9\text{Be}(^3\text{He},n)^{11}\text{C}$  reaction, agreed with the integral data obtained in this work. The distorted-wave theory of direct reactions was used to compute excitation functions for comparison with integral data for  $(^3\text{He},\alpha)$  reactions on  $^{12}\text{C}$ ,  $^{16}\text{O}$ , and  $^{19}\text{F}$ , and for the  $(^3\text{He},d)$  reaction on  $^{12}\text{C}$ . The results of the comparison between theory and experiment indicate that a direct mechanism is operative in all the cases studied, except the  $^{12}\text{C}(^3\text{He},\alpha)^{11}\text{C}$  reaction, which appears to proceed to a large extent by way of a compound-nucleus reaction. Thus, the integral data indicate that the primary mechanisms operative in the reactions  $(^3\text{He},\alpha)$  on  $^{16}\text{O}$  and  $^{19}\text{F}$ , and  $(^3\text{He},d)$  on  $^{12}\text{C}$ , are respectively direct pickup and stripping.

### I. INTRODUCTION

NUCLEAR reactions initiated by  $^3\text{He}$  particles have received much attention during the past few years. Such simple reactions as  $(^3\text{He},n)$ ,  $(^3\text{He},p)$ ,  $(^3\text{He},d)$ , and  $(^3\text{He},\alpha)$  have been studied in many experiments in which the variations of the differential cross section with angle and energy have been determined for discrete nuclear states by counting the particles emitted in the reaction. The results of these studies have contributed much to our knowledge of nuclear structure and of nuclear reactions.<sup>1,2</sup> In particular, data from simple reactions of  $^3\text{He}$  particles with low- $Z$  elements,<sup>3-15</sup> usually leading to low-lying states in

the product nuclei, have been successfully analyzed in terms of direct-interaction theories of nuclear reactions.

<sup>4</sup> D. R. Osgood, J. R. Patterson, and E. W. Titterton, Nucl. Phys. **60**, 503 (1964).

<sup>5</sup> J. H. Towle and B. E. F. Macefield, Proc. Phys. Soc. (London) **77**, 399 (1961).

<sup>6</sup> G. U. Din, H. M. Kuan, and T. W. Bonner, Nucl. Phys. **50**, 267 (1964).

<sup>7</sup> I. J. Taylor, F. de S. Barros, P. D. Forsyth, A. A. Jaffe, and S. Ramavataram, Proc. Phys. Soc. (London) **75**, 772 (1960).

<sup>8</sup> S. Hinds and R. Middleton, Proc. Phys. Soc. (London) **75**, 745 (1960).

<sup>9</sup> H. M. Kuan, T. W. Bonner, and J. R. Risser, Nucl. Phys. **51**, 481 (1964).

<sup>10</sup> H. C. Bryant, J. G. Beery, E. R. Flynn, and W. T. Leland, Nucl. Phys. **53**, 97 (1964).

<sup>11</sup> S. Hinds and R. Middleton, Proc. Phys. Soc. (London) **74**, 775 (1959).

<sup>12</sup> S. Hinds and B. M. Hinds, Nucl. Phys. **48**, 690 (1963).

<sup>13</sup> W. P. Alford, L. M. Blau, and D. Cline, Nucl. Phys. **61**, 368 (1965).

<sup>14</sup> W. P. Alford, L. M. Blau, and D. Cline, University of Rochester Report No. UR-875-65, 1964 (unpublished).

<sup>15</sup> R. H. Siemssen, L. L. Lee, Jr., and D. Cline, Phys. Rev. **140**, B1258 (1965).

<sup>†</sup> Research sponsored by the U. S. Atomic Energy Commission under contract with the Union Carbide Corporation.

<sup>1</sup> *Direct Interactions and Nuclear Reaction Mechanisms*, edited by E. Clementel and C. Villi (Gordon and Breach Science Publishers, Inc., New York, 1962).

<sup>2</sup> Argonne National Laboratory Report No. ANL-6878, 1964 (unpublished).

<sup>3</sup> J. H. Towle and B. E. F. Macefield, Nucl. Phys. **66**, 65 (1965).

However, relatively few papers have appeared in the literature concerning integral measurements (wherein cross sections are measured by assay of radioactive product nuclei) with  $^3\text{He}$  particles and low- $Z$  elements.<sup>16-19</sup> Nevertheless, such experiments are of interest because they test whether the success of the theory of direct interactions in explaining differential data can be duplicated with respect to integral measurements. This question is not a trivial one, for the results from the two types of measurements may not always be consistent.<sup>20</sup> In an integral experiment, the cross section represents a sum (often over angles) of the contributions of all states in the product nucleus up to the separation energy,  $S$ , of the most loosely bound particle in that nuclide. This sum may, in addition, contain terms due to states above  $S$  that decay by  $\gamma$ -ray, rather than particle, emission. In contrast, differential particle-counting experiments do not often detect all of the states below  $S$ . So, what is observed for a few low-energy states in the differential experiment may not be representative of the reactions seen in the integral study. For example, compound-nucleus, instead of direct, reactions may tend to predominate for those transitions that lead to states near  $S$ .

In this paper, experimental integral excitation functions for reactions of  $^3\text{He}$  particles of 3 to 10 MeV with beryllium, carbon, oxygen, and fluorine are reported. To investigate the questions raised above of consistency of experimental data and of interpretation in terms of nuclear reaction mechanisms, our results are compared with excitation functions measured in differential studies or calculated with the distorted-wave theory of direct reactions.<sup>21</sup>

## II. EXPERIMENTAL PROCEDURE

### A. Irradiations

The irradiations were performed at the ORNL 5.5-MeV Van de Graaff accelerator. The kinetic energy of the particles from this machine can be continuously varied, with a maximum energy resolution of about 5 keV. Energies up to 10 MeV were attainable by acceleration of doubly ionized  $^3\text{He}$  particles. The highest beam currents available were about 0.05  $\mu\text{A}$ . The targets used and their thicknesses were beryllium, 0.0005 in., Teflon (C,F), 0.00025 in., Mylar (C,H,O), 0.00025 and 0.0005 in., and nylon (C,H,O,N), 0.00075 in. Routine chemical analyses were performed to determine the composition of the plastics. To com-

<sup>16</sup> J. D. Mahony, University of California Report No. UCRL-11780, 1965 (unpublished); S. S. Markowitz and J. D. Mahony, *Anal. Chem.* **34**, 329 (1962).

<sup>17</sup> D. R. F. Cochran and J. D. Knight, *Phys. Rev.* **128**, 1281 (1962).

<sup>18</sup> O. D. Brill, *Soviet J. Nucl. Phys.* **1**, 37 (1965).

<sup>19</sup> A. S. Chohan, *J. Nat. Sci. Math.* **4**, 65 (1964).

<sup>20</sup> This point has been discussed by N. T. Porile, *Phys. Rev.* **121**, 184 (1961).

<sup>21</sup> R. H. Bassel, R. M. Drisko, and G. R. Satchler, Oak Ridge National Laboratory Report No. ORNL-3240, 1962 (unpublished).

TABLE I. Decay-scheme parameters of detected radionuclides.\*

Radio-nuclide	Half-life	Energy (MeV) and % of emitted radiation per decay	
		Positrons	$\gamma$ Rays
$^{11}\text{C}$	20.5 min	0.96 (100%)	None
$^{13}\text{N}$	10.0 min	1.19 (100%)	None
$^{14}\text{O}$	72 sec	1.81 (99.4%)	2.31 (99.4%)
		4.14 (0.6%)	
$^{15}\text{O}$	124 sec	1.74 (100%)	None
$^{17}\text{F}$	66 sec	1.74 (100%)	None
$^{18}\text{F}$	110 min	0.65 (97%)	None

\* Reference 25.

pensate for the loss of radioactive nuclei by recoil from a given target, a sandwich of three identical plastic foils was irradiated at each desired  $^3\text{He}$  energy. The target in the middle of the sandwich was then assayed for radioactivity. Kinematic calculations show that backward recoil, i.e., at angles larger than  $90^\circ$  with respect to the direction of the  $^3\text{He}$  beam, cannot occur in the beryllium targets at the  $^3\text{He}$  energies used. Therefore, a single gold foil, thicker than the range of the recoiling nuclei, was attached to each of the beryllium foils to stop the recoils in the forward direction. The absolute activities of the gold catchers at end of bombardment were added to those of their corresponding beryllium targets, to calculate the final results.

The target assembly, insulated from the remainder of the accelerator, served as a Faraday cup that, after proper calibration, was used to measure the intensity of the  $^3\text{He}$  beam. The various targets were all irradiated in the machine vacuum with the target holder held against the end of the beam pipe by the vacuum, so that the targets could be rapidly removed for assay of radioactivity after irradiation. Depending upon the half-lives of the desired products, the targets were bombarded for either 1 or 10 min.

### B. Counting

All of the radioactive nuclides that were produced in the  $^3\text{He}$  irradiations of beryllium, carbon, nitrogen, oxygen, and fluorine are positron emitters. Some of the decay-scheme parameters of these radionuclides are presented in Table I.

Gamma-ray spectrometry was used to determine the absolute disintegration rates of all the targets. Hence, the 0.511-MeV  $\gamma$  rays arising from the annihilation of the positrons were counted. Copper disks, sufficiently thick to ensure complete annihilation of all the emitted positrons, were accordingly placed on each side of each positron-emitting sample. The 2.31-MeV  $\gamma$ -ray of  $^{14}\text{O}$  was also counted. The  $\gamma$  rays were detected with a  $3 \times 3$  in. NaI(Tl) detector, connected to a multichannel analyzer. No chemical separations were performed in these experiments. The various targets were simply counted at either 10 or 20 cm from the detector. Decay-curve analysis of the counting data, performed by the

method of least squares with the CLSQ code<sup>22</sup> on the IBM 7090 computer, served to separate the contributions of the various radioactive products. The counting rate due to a given  $\gamma$  ray was obtained by fitting a Gaussian shape to the experimental  $\gamma$ -ray peak and then calculating its area. Calculated efficiency factors<sup>23</sup> were used to convert counting rates to disintegration rates. Correction was made for summing between the positron annihilation radiation and the 2.31-MeV  $\gamma$  ray emitted in coincidence in the decay of  $^{14}\text{O}$ .

The counting rates due to  $^{14}\text{O}$  and  $^{17}\text{F}$ , which have very similar half-lives, could be resolved because of the 2.31-MeV  $\gamma$  ray of  $^{14}\text{O}$ . A typical  $\gamma$ -ray spectrum, from a sample containing  $^{14}\text{O}$  as well as the other nuclides listed in Table I, is shown in Fig. 1. By following the decay of the 2.31-MeV  $\gamma$ -ray, we determined the contribution of  $^{14}\text{O}$  to the 0.511-MeV peak. The least-squares code subtracted this contribution from the decay curve and then analyzed the decay of the other components under the 0.511-MeV peak. To check the accuracy of the least-squares analysis program, we prepared several exact decay curves by combining the intensities for the six given components, calculated from the law of radioactive decay. The computer analysis of the artificial decay curves was carried out with the  $^{14}\text{O}$  intensity as part of the input data. The results of the computer calculations were in excellent agreement with the "true" intensities, demonstrating that the program can successfully treat components whose half-lives differ by a factor of about 2 or greater.

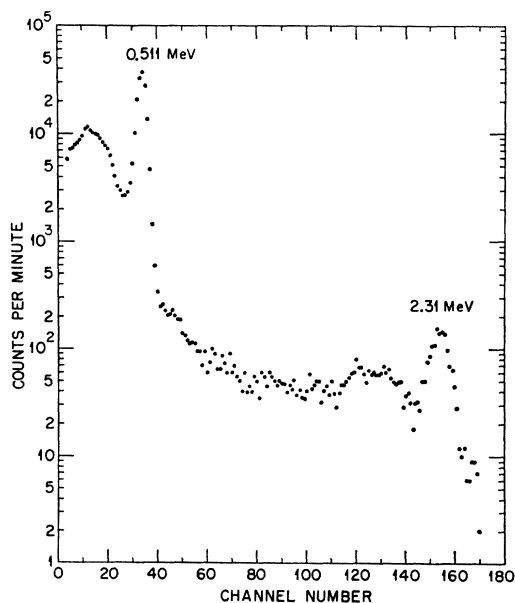


Fig. 1. Typical  $\gamma$ -ray spectrum of a sample containing all the nuclides listed in Table I.

<sup>22</sup> J. B. Cumming, Natl. Acad. Sci.—Natl. Research Council, Nucl. Sci. Ser. NAS-NS 3107, 25 (1963).

<sup>23</sup> R. L. Heath, U. S. Atomic Energy Commission Report No. IDO-16880, 1964 (unpublished).

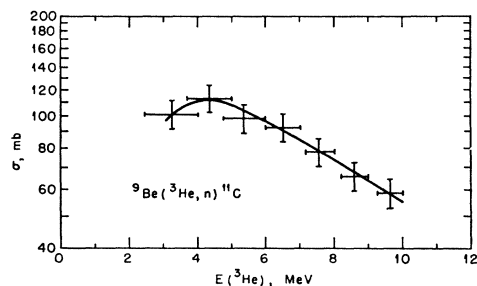


FIG. 2. Excitation function for the reaction  $^9\text{Be}(^3\text{He},n)^{11}\text{C}$ .

### III. RESULTS

Since no enriched isotopes were used in these experiments, the production of a particular radionuclide by irradiation of an element could be due to nuclear reactions induced in different isotopes. However, each of the elements involved has a major constituent of isotopic abundance greater than 98.8%; therefore, the production of a radionuclide will be attributed in all cases to the most abundant isotope of the irradiated element. Also, radioactive decay of a precursor may lead to the nuclide being assayed; only the reaction leading directly to this nuclide will be mentioned in these cases. Thus, for example, only the reaction  $^{16}\text{O}(^3\text{He},p)^{18}\text{F}$  will be listed to account for all the processes capable of producing  $^{18}\text{F}$  from oxygen, i.e.,  $^{17}\text{O}(^3\text{He},d)^{18}\text{F}$ ,  $^{17}\text{O}(^3\text{He},pn)^{18}\text{F}$ ,  $^{17}\text{O}(^3\text{He},2n)^{18}\text{Ne} \rightarrow ^{18}\text{F}$ ,  $^{16}\text{O}(^3\text{He},p)^{18}\text{F}$ , and  $^{16}\text{O}(^3\text{He},n)^{18}\text{Ne} \rightarrow ^{18}\text{F}$ .

The excitation functions obtained in these experiments are presented in Table II and Figs. 2 to 6. The errors listed in Table II, represented by the vertical bars in the figures, are attributed to counting statistics, decay-curve analysis, and to uncertainties in decay parameters, counting efficiencies, Faraday-cup readings, and target composition and thickness. The errors due to counting statistics and decay-curve analysis combined were normally obtained in the form of standard deviations from the output of the CLSQ program.<sup>22</sup> These errors were then propagated with an estimated over-all error of  $\pm 10\%$  attributed to all the other effects, except for the nylon irradiations. Here, the over-all error was estimated to be  $\pm 15\%$ , because variations of thickness of the nylon foil were larger than those found in the other foils. The energy intervals in Table II correspond to the kinetic energies of the  $^3\text{He}$  ions that enter and leave a particular target foil; these two energies reflect the degradation of the  $^3\text{He}$  energy, caused successively by the first recoil-catcher foil, and by the target foil itself. To calculate these energy intervals, range-energy curves were constructed for the different targets from existing range-energy data<sup>24</sup> for hydrogen, beryllium, carbon, nitrogen, oxygen, and fluorine. The horizontal bars in the excitation curves

<sup>24</sup> C. Williamson and J. P. Boujot, Commissariat à l'Énergie Atomique Report No. 2189, 1962 (unpublished).

TABLE II. Cross sections (in mb) for  $^3\text{He}$  nuclear reactions induced in beryllium, carbon, oxygen, and fluorine.

Mid-energy interval (MeV)	Energy interval (MeV)	$^9\text{Be}(^3\text{He},n)^{11}\text{C}$	$^{12}\text{C}(^3\text{He},n)^{14}\text{O}$	$^{12}\text{C}(^3\text{He},d)^{13}\text{N}$	$^{12}\text{C}(^3\text{He},\alpha)^{11}\text{C}$	$^{16}\text{O}(^3\text{He},p)^{18}\text{F}$	$^{16}\text{O}(^3\text{He},\alpha)^{15}\text{O}$	$^{19}\text{F}(^3\text{He},\alpha)^{18}\text{F}$	$^{19}\text{F}(^3\text{He},\alpha n)^{17}\text{F}$
2.4	3.0-1.8		11.2 $\pm$ 1.4		118 $\pm$ 14				
2.9	3.4-2.4		6.99 $\pm$ 0.74		103 $\pm$ 7				
3.2	4.0-2.4	102 $\pm$ 10							
3.7	4.2-3.2		4.50 $\pm$ 0.48		135 $\pm$ 21				
4.1	4.4-3.8		8.66 $\pm$ 0.92		153 $\pm$ 11				
4.3	5.0-3.7	113 $\pm$ 11							
4.9	5.3-4.5		12.8 $\pm$ 1.5		256 $\pm$ 18				
5.2	5.5-4.9		13.4 $\pm$ 1.3		182 $\pm$ 13				
5.4	6.0-4.8	98.6 $\pm$ 9.9							
6.0	6.4-5.7		11.3 $\pm$ 1.3	32.9 $\pm$ 3.9	268 $\pm$ 19				
6.3	6.6-6.1		16.5 $\pm$ 1.8	46.2 $\pm$ 6.4	218 $\pm$ 27				
6.5	7.0-6.0	93.0 $\pm$ 9.3							
6.6	7.1-6.1		13.9 $\pm$ 1.4	59.6 $\pm$ 8.4	278 $\pm$ 39				
7.1	7.4-6.8		8.60 $\pm$ 0.97	56.6 $\pm$ 5.0	329 $\pm$ 23				
7.2	8.0-6.3								
7.6	8.0-7.1	78.0 $\pm$ 7.8							
7.8	8.2-7.3		12.1 $\pm$ 1.3	56.5 $\pm$ 8.4	289 $\pm$ 29				
8.2	8.5-8.0		13.6 $\pm$ 1.6	81.1 $\pm$ 6.9	366 $\pm$ 26				
8.4	9.1-7.8								
8.6	9.0-8.2	65.8 $\pm$ 6.6							
8.9	9.3-8.5		10.2 $\pm$ 1.0	61.8 $\pm$ 8.8	349 $\pm$ 26				
9.3	9.6-9.1		7.72 $\pm$ 0.83	60.8 $\pm$ 6.0	331 $\pm$ 23				
9.5	9.7-9.3			98.9 $\pm$ 12.2	308 $\pm$ 31				
9.6	10.0-9.3	58.7 $\pm$ 5.9							

represent the energy intervals of Table II, and also account for small uncertainties in target thickness.

Results for the reactions  $^{12}\text{C}(^3\text{He},\alpha)^{11}\text{C}$  and  $^{12}\text{C}(^3\text{He},d)^{13}\text{N}$  are plotted in Fig. 3. Counting of  $^{11}\text{C}$  and  $^{13}\text{N}$  could normally be performed with satisfactory precision after the 1-min irradiations. Another set of data for the same nuclides was obtained in the 10-min irradiations of the same plastics. Therefore, several averaged, low-error values were calculated for the reactions presented in Fig. 3. It should be noted, however, that the averaged points at 4.9 MeV (from a Teflon irradiation) and at 5.2 MeV (Mylar), of  $^{12}\text{C}(^3\text{He},\alpha)^{11}\text{C}$ , do not fall on the smooth curve. The same is true for the points (Teflon) at 8.2 and 9.3 MeV of  $^{12}\text{C}(^3\text{He},d)^{13}\text{N}$ . Loss of  $^{11}\text{C}$  and  $^{13}\text{N}$  as gaseous products could be an explanation for the above discrepancies. However, experiments conducted by Cochran and Knight<sup>17</sup> and by Mahony<sup>16</sup> showed that no more than 5% of  $^{11}\text{C}$ ,  $^{13}\text{N}$ , and  $^{18}\text{F}$  formed in polyethylene, Mylar, and Teflon foils was lost in irradiations with  $^3\text{He}$  particles. The noted irregularities in cross section may be due to fine structure in the excitation functions for the reactions  $^{12}\text{C}(^3\text{He},\alpha)^{11}\text{C}$  and  $^{12}\text{C}(^3\text{He},d)^{13}\text{N}$ .

Figure 3 also presents a comparison of our data for the above reactions and those of Cochran and Knight<sup>17</sup> and Mahony.<sup>16</sup> These authors used the stacked-foil technique in their experiments. However, Mahony stacked enough foils and catchers to attenuate a 31-MeV  $^3\text{He}$  beam completely, while Cochran and Knight irradiated different foil stacks at selected  $^3\text{He}$  energies, the lowest of which was 10 MeV. The energy uncertainties, associated with large beam-energy degradations, could be one of the causes of the difference between

Mahony's results for the reaction  $^{12}\text{C}(^3\text{He},\alpha)^{11}\text{C}$  and those of Cochran and Knight and this work. The same argument can be applied to the comparisons with Mahony's data shown in Figs. 5 and 6 for other nuclear reactions. It must be noted that in general the shapes and values of the curves agree within experimental errors, and that only a shift in energy would be required to make the agreement more satisfactory.

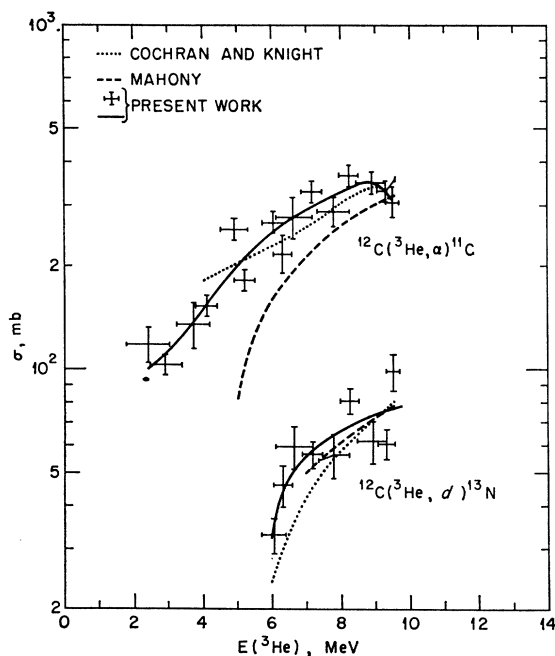


FIG. 3. Excitation functions for the reactions  $^{12}\text{C}(^3\text{He},\alpha)^{11}\text{C}$  and  $^{12}\text{C}(^3\text{He},d)^{13}\text{N}$ . Comparison with the data from Refs. 16 and 17.

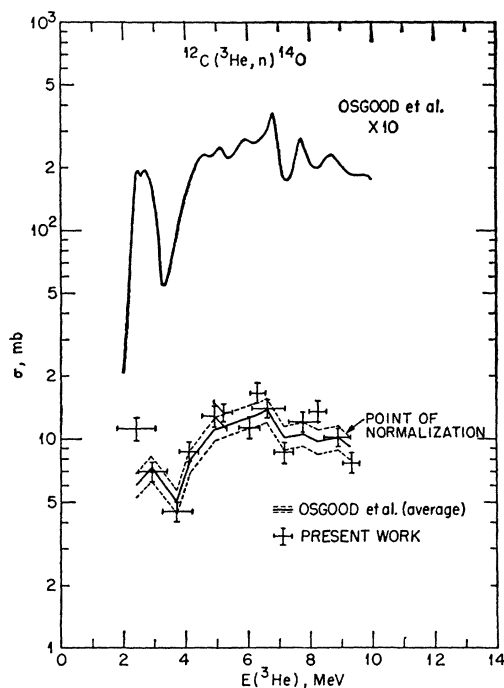


FIG. 4. Excitation function for the reaction  $^{12}\text{C}(^3\text{He},n)^{14}\text{O}$ . Comparison with data from Ref. 4.

Our  $^{12}\text{C}(^3\text{He},d)^{13}\text{N}$  curve was determined by irradiating Teflon and Mylar foils. The contribution of the interfering reaction  $^{19}\text{F}(^3\text{He},n2\alpha)^{18}\text{N}$  was neglected because, although its threshold is 5.6 MeV, the values from Teflon targets (e.g., points at 8.2 and 9.3 MeV) are in general agreement with those obtained from Mylar, and with the curves of Cochran and Knight and Mahony, who used fluorine-free plastics in their experiments.

Figure 4 shows a comparison between our data for the reaction  $^{12}\text{C}(^3\text{He},n)^{14}\text{O}$  and the excitation function (upper curve) determined for this reaction by Osgood *et al.*<sup>4</sup> by irradiating very thin foils. To make a valid comparison, we constructed an excitation function by averaging cross-section values from the upper curve over the energy intervals corresponding to our data points. This curve (solid line) is compared with our data in the lower part of Fig. 4; the dashed lines indicate the error band for the data of Ref. 4. This comparison shows that our data strongly support the fine structure found by Osgood *et al.* It must be noted, however, that there is approximately a factor of 2.4 difference between the absolute cross-section values of both curves. In fact, the data of Ref. 4 were normalized to our values at the 8.9-MeV point. Possible systematic errors in Faraday-cup readings and counting-efficiency factors may be responsible for this difference. However, it should be noted that we normally assayed a given target of Teflon or Mylar not only for  $^{14}\text{O}$ , but also for  $^{11}\text{C}$  and  $^{13}\text{N}$  formed during the same irradiation. We have already shown in the discussion of Fig. 3 that the

results related to the latter two nuclides are in reasonable agreement with published data.

The excitation function for the reaction  $^{16}\text{O}(^3\text{He},\alpha)^{15}\text{O}$ , shown in Fig. 5, was obtained from irradiations of Mylar foils. Possible interference from the reaction  $^{12}\text{C}(^3\text{He},\gamma)^{15}\text{O}$  was ruled out because no  $^{15}\text{O}$  was found in any of the irradiated Teflon targets. A few isolated cross-section values were also obtained in these experiments. Two points were determined for the reaction  $^{16}\text{O}(^3\text{He},d)^{17}\text{F}$  by irradiating Mylar foils:  $79 \pm 19$  mb at 7.8 MeV, and  $60 \pm 23$  mb at 8.9 MeV. Also, experiments with nylon foils showed that the reaction  $^{14}\text{N}(^3\text{He},d)^{15}\text{O}$  has a cross section of about 80 mb at 7–8 MeV while the cross section for the reaction  $^{14}\text{N}(^3\text{He},\alpha)^{13}\text{N}$  at 1.5–3 MeV is about 20 mb. Mahony<sup>16</sup> found roughly the same value for the latter reaction. The errors of these determinations are large, not only because of the nylon-foil thickness uncertainties, but also due to the respectively interfering reactions,  $^{16}\text{O}(^3\text{He},\alpha)^{15}\text{O}$  and  $^{12}\text{C}(^3\text{He},d)^{13}\text{N}$ , whose effects had to be subtracted in the calculations.

#### IV. DISCUSSION

##### A. Comparison of Differential and Integral Data. The $^9\text{Be}(^3\text{He},n)^{11}\text{C}$ Reaction

Before proceeding to a comparison of direct-interaction theory with our experimental results, it seems appropriate to demonstrate the essential agreement

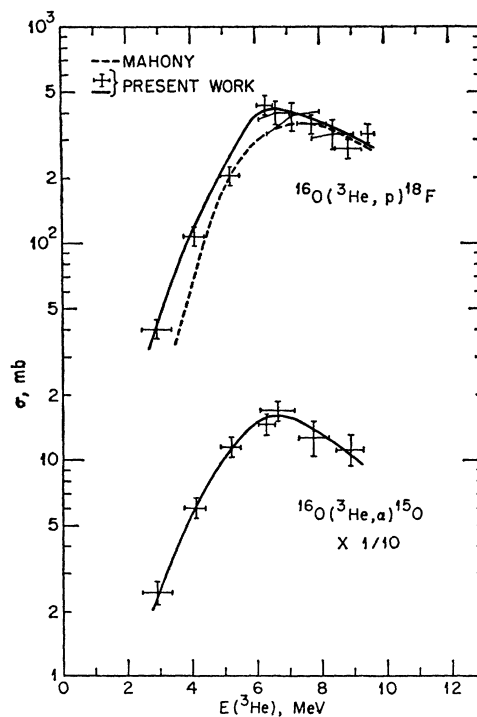


FIG. 5. Excitation functions for the reactions  $^{16}\text{O}(^3\text{He},p)^{18}\text{F}$  and  $^{16}\text{O}(^3\text{He},\alpha)^{15}\text{O}$ . Comparison of the upper curve with data from Ref. 16.

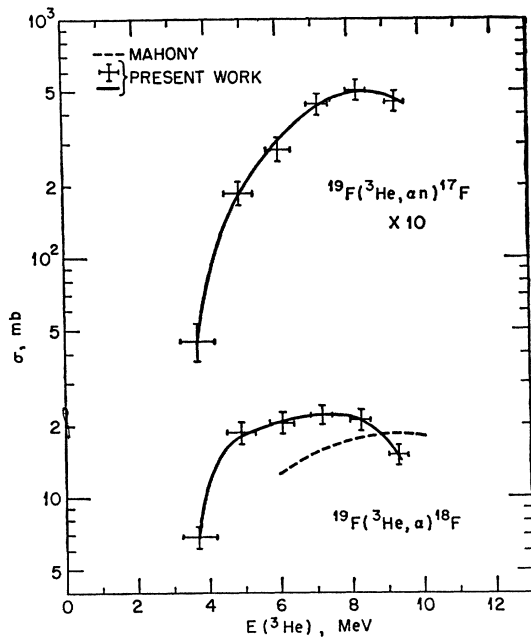


FIG. 6. Excitation functions for the reactions  $^{19}\text{F}(^3\text{He}, \alpha n)^{17}\text{F}$  and  $^{19}\text{F}(^3\text{He}, \alpha)^{18}\text{F}$ . Comparison of the lower curve with data from Ref. 16.

between differential and integral results for a reaction that has been successfully described in terms of the theory. The differential-cross-section data of Towle and Macefield,<sup>3</sup> for the  $^9\text{Be}(^3\text{He}, n)^{11}\text{C}$  reaction at  $^3\text{He}$  energies between 3.5 and 5.8 MeV, are ideally suited for a detailed comparison with our integral excitation function. In their work, neutron groups leading to all the states of  $^{11}\text{C}$  from 0 to 8.1 MeV were detected. The respective separation energies of  $\alpha$  particles and protons from  $^{11}\text{C}$  are 7.5 and 8.7 MeV,<sup>26</sup> so that the states observed were essentially all those that are stable to further particle emission. So, unless our integral results contain appreciable contributions from those states above 8.1 MeV that have been observed to decay by  $\gamma$ -ray emission,<sup>25</sup> we may expect that the data from the differential and integral studies will agree.

To compare the two sets of measurements, we used the differential cross sections<sup>3</sup> to construct an integral excitation function. The data so used consisted, for each state,  $n$ , observed in  $^{11}\text{C}$ , of excitation functions taken at  $5^\circ$  in the laboratory system [curves of  $\sigma_n(5^\circ, \text{lab})$ -versus- $^3\text{He}$ -ion energy], and angular distributions in the center-of-mass system [curves of  $\sigma_n(\theta)$ -versus-c.m. angle  $\theta$ ] measured at  $^3\text{He}$  energies of 4.2 and 5.2 MeV. To get the total cross section,  $\sigma_{tn}$ , for each  $^{11}\text{C}$  state, we integrated the angular distributions,

$$\sigma_{tn} = 2\pi \int_0^\pi \sigma_n(\theta) \sin\theta \, d\theta. \quad (1)$$

<sup>25</sup> T. Lauritsen and F. Ajzenberg-Selove, in *Nuclear Data Sheets*, compiled by K. Way *et al.* (National Academy of Sciences—National Research Council, Washington, D. C., 1962), NRC 61-5, 6-119, 171, 197, 215, 255, 267.

Because the angular distributions were measured to only  $\sim 132^\circ$ , the curves were extrapolated to  $180^\circ$ . Then, to determine the energy dependence of  $\sigma_{tn}$ ,  $\sigma_n(5^\circ, \text{lab})$  was transformed into the c.m. system,<sup>26</sup> giving  $\sigma_n(\theta_0)$ , where  $\theta_0$  is the particular c.m. angle corresponding to  $5^\circ$  lab at each energy of interest. We assumed that the shapes of the angular distributions varied very slowly with energy, so that, in the observed energy range, the ratio of  $\sigma_{tn}/\sigma_n(\theta_0)$  determined at 5.2 MeV, was taken to be constant; using this ratio and the various  $\sigma_n(\theta_0)$  values, we calculated  $\sigma_{tn}$  at different energies. Summing over the  $n$  states, from 0 to 8.1 MeV, thus gave an integral excitation function that could be directly compared with our data. Repeating the calculations with the assumption that the angular distributions at 4.2 MeV were representative of all energies of interest gave cross-section values  $\sim 28\%$  higher than those obtained with the curves at 5.2 MeV as standards. Thus, the assumption of the energy independence of the angular distributions is not grossly incorrect. As shown in Fig. 7, the integrated data of Towle and Macefield agree with our results within the errors of the respective measurements. Although this result depends upon the specific extrapolations and approximations made, the general agreement in shape and magnitude demonstrates the essential consistency of the differential and integral measurements.

In their paper, Towle and Macefield were able to fit the shapes of most of their angular distributions by using a distorted-wave direct-interaction model in which two protons are transferred from the  $^3\text{He}$  particle to the  $^9\text{Be}$  nucleus.<sup>27</sup> The main shortcoming of the theoretical calculation is that, while it did fit the large observed forward peak in the angular distributions, it underestimated the magnitudes of the smaller peaks observed at large angles. Normalization of the calculations to the data points was also necessary<sup>3</sup> because the theory did not predict the values of the cross sections. We combined their normalized theoretical angular distributions at 5.2 MeV to get a value of the integrated cross section at that energy. This value is seen in Fig. 7 to account for  $\sim 50\%$  of the integrated excitation function (solid line).

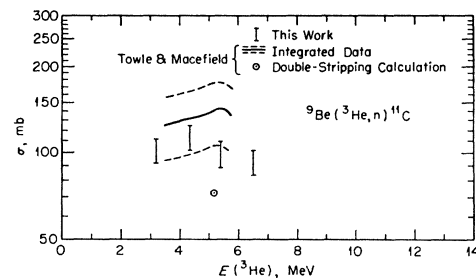


FIG. 7. The  $^9\text{Be}(^3\text{He}, n)^{11}\text{C}$  reaction. Comparison of the integrated results from Ref. 3 with the data from this work.

<sup>26</sup> J. B. Ball, Oak Ridge National Laboratory Report No. ORNL-3251, 1962 (unpublished).

<sup>27</sup> J. R. Rook and D. Mitra, *Nucl. Phys.* **51**, 96 (1964).

That the cross sections calculated with the direct-reaction theory are significant in the  ${}^9\text{Be}({}^3\text{He},n){}^{11}\text{C}$  case, where the differential and integral data demonstrably agree, served as justification for our applying the theory to other reactions in which, at the most, differential data exist for only a few low-lying states. The theory itself was used to compute the contributions of the various states of interest and to give us calculated integral excitation functions for comparison with our experimental results.

### B. Comparison of Distorted-Wave Theory with Integral Data

The form of the distorted-wave (DW) theory that we used is that of Bassel, Drisko, and Satchler.<sup>21</sup> Calculations were performed with their code, JULIE, on the IBM 7090 computer, for  $({}^3\text{He},\alpha)$  and  $({}^3\text{He},d)$  reactions, in which a single nucleon is either picked-up by, or stripped from, the  ${}^3\text{He}$  particle. The quantity of interest calculated with this code is  $\sigma_{lsj}(\theta)$ , the reduced cross section for the transferred nucleon, with orbital angular momentum  $l$ , spin  $s$ , and total angular momentum  $j$ . This reduced cross section is related to the differential cross section,  $d\sigma(\theta)/d\Omega$ , by the following relations: For pickup,  $({}^3\text{He},\alpha)$ ,

$$\frac{d\sigma(\theta)}{d\Omega} = \left( \frac{2s_\alpha + 1}{2s_h + 1} \right) \left( \frac{N}{2s + 1} \right) \sum_{ij} S(lj) \sigma_{lsj}(\theta), \quad (2)$$

where  $s$ ,  $s_\alpha$ , and  $s_h$  are the spins of the transferred neutron, the  $\alpha$ , and the  ${}^3\text{He}$  particles, respectively;  $N$  is a factor that includes the strength of the nuclear interaction and the overlap for the formation of the  $\alpha$  particle from  ${}^3\text{He}+n$ ; and  $S(lj)$  is the spectroscopic factor<sup>28,29</sup> for the state  $(lj)$ . For stripping,  $({}^3\text{He},d)$ ,

$$\frac{d\sigma(\theta)}{d\Omega} = \left( \frac{2J_f + 1}{2J_i + 1} \right) \left( \frac{N}{2s + 1} \right) \sum_{ij} S(lj) \sigma_{lsj}(\theta), \quad (3)$$

where  $J_i$  and  $J_f$  are the spins of the initial and final nuclei;  $s$  is the spin of the transferred proton; and  $N$  is the overlap factor between  ${}^3\text{He}$  and  $d+p$ . Often, only one value of  $lj$  is important in a given transition, so no summation over  $l$  and  $j$  is necessary in Eqs. (2) and (3). After the theoretical values of  $d\sigma(\theta)/d\Omega$  were obtained, integration over  $\theta$  and summation over the different nuclear states, as described previously, resulted in an integral excitation function.

In computing  $\sigma_{lsj}(\theta)$ , we had to describe the interaction in terms of optical-model parameters for the entrance and exit channels and in terms of the wave function of the transferred nucleon. The nucleon wave function was generated with a Woods-Saxon potential

with the following parameters: radius of the potential well, 1.25 F; charge radius, 1 F; diffuseness, 0.65 F. The depth of the well was also adjusted to fit the observed binding energy of the transferred nucleon in the nucleus of interest. To maintain some connection with reality in this comparison of theory with experiment, we used, whenever possible, optical-model parameters that had previously been determined in differential studies of the particular reaction being considered. Our computational procedure, then, did not allow for the variation of any input parameters.

### The ${}^{16}\text{O}({}^3\text{He},\alpha){}^{15}\text{O}$ Reaction

Alford *et al.*<sup>13,14</sup> have investigated this reaction for the transition to the  ${}^{15}\text{O}$  ground state at  ${}^3\text{He}$  energies of 8–10 MeV. Using the DW theory, they obtained reasonable fits to the shapes of their angular distributions, but were not able to reproduce the magnitudes of the cross sections. That is, they found, with a value of  $N$  of 6.53 calculated from the interaction of  ${}^3\text{He}$  and  $n$ , that their theoretical cross sections were low by a factor of  $24 \pm 5$ . Similar results were obtained in studies from 8 to 11 MeV of  $({}^3\text{He},\alpha)$  reactions<sup>30,31</sup> on  ${}^{40}\text{Ca}$  and  ${}^{39}\text{K}$ . This constant, large factor needed to normalize theory to experiment has been explained<sup>32</sup> as being due to our scant knowledge of the  $\alpha$ -particle wave function. Hence, an error arises in the evaluation of  $N$ , the overlap factor between  $\alpha$  and  ${}^3\text{He}+n$ , that is independent of the properties of the nuclear states involved in the reaction, and depends only upon the fact that the reaction is of the type  $({}^3\text{He},\alpha)$ .

In calculating the integral cross section from the DW theory, it would be ideal to include all the states in the final nucleus below the threshold for particle emission. However, this task is complicated by the fact that some of the states are not pure shell-model states, but instead involve the mixing of several configurations. In  ${}^{15}\text{O}$ , the negative-parity states at 0 and 6.16 MeV can be written as  $(p_{1/2})^{-1}$  and  $(p_{3/2})^{-1}$  configurations, respectively; the  $({}^3\text{He},\alpha)$  reaction leading to the 0- (or 6.16-) MeV state simply involves  $l=1$  pick-up of a  $p_{1/2}$  (or  $p_{3/2}$ ) neutron from the closed  $s^4p^{12}$  core of  ${}^{16}\text{O}$ . But transitions to the positive-parity states in  ${}^{15}\text{O}$  cannot be explained so simply. For example, the  $J=\frac{1}{2}^+$  states have been described as being mixtures of  $s^3p^{12} + s^4p^{10}d + s^4p^{10}s$  configurations.<sup>33</sup> Calculation of cross sections and spectroscopic factors for such mixtures is difficult. However, recent investigations of the  ${}^{16}\text{O}({}^3\text{He},\alpha){}^{15}\text{O}$  reaction<sup>34</sup> and the  ${}^{16}\text{O}(d,{}^3\text{He}){}^{15}\text{N}$  reaction<sup>35</sup>

<sup>30</sup> D. Cline, L. M. Blau, and W. P. Alford, Nucl. Phys. **73**, 33 (1965).

<sup>31</sup> L. M. Blau, W. P. Alford, D. Cline, and H. E. Gove, University of Rochester Report No. UR-875-90, 1965 (unpublished).

<sup>32</sup> R. H. Bassel (private communication).

<sup>33</sup> E. C. Halbert and J. B. French, Phys. Rev. **105**, 1563 (1957).

<sup>34</sup> E. K. Warburton, P. D. Parker, and P. F. Donovan, Phys. Letters **19**, 397 (1965).

<sup>35</sup> J. C. Hiebert, E. Newman, and R. H. Bassel, Bull. Am. Phys. Soc. **11**, 44 (1966).

<sup>28</sup> M. H. Macfarlane and J. B. French, Rev. Mod. Phys. **32**, 567 (1960).

<sup>29</sup> J. B. French, in *Nuclear Spectroscopy*, edited by F. Ajzenberg-Selove (Academic Press Inc., New York, 1960), Part B, pp. 890–931.

TABLE III. Optical-model parameters used in distorted-wave calculations.<sup>a</sup>

Reaction partners	Entrance channel							Reaction partners	Exit channel								
	$V$	$W$	$r_0$	$r_c$	$a$	$r_w$	$a_w$		$V$	$W$	$r_0$	$r_c$	$a$	$V_{so}$	$r_w$	$a_w$	$\tau$
$^{16}\text{O}+^3\text{He}^b$	171.5	13.9	1.03	1.4	0.893	2.06	0.508	$^{16}\text{O}+\alpha^b$	111	6.5	1.4	1.4	0.6				
$^{19}\text{F}+^3\text{He}^c$								$^{18}\text{F}+\alpha$									
$^{12}\text{C}+^3\text{He}^d$								71									
	$^{13}\text{N}+d^e$	93	0	1	1.3	1.047											

<sup>a</sup> For definitions of the parameters, see Ref. 21.  $V$  and  $W$  are given in MeV;  $r$  and  $a$  in F.

<sup>b</sup> See Refs. 13 and 14. A cutoff radius of 4.3 F was used.

<sup>c</sup> For a discussion of the similarities in the parameters for  $^{16}\text{O}$  and  $^{19}\text{F}$ , see Ref. 15. Cutoff radius = 4.3 F.

<sup>d</sup> See Ref. 35. Cutoff radius = 3.1 F.

<sup>e</sup> These parameters were suggested by R. H. Bassel (private communication). No cutoff radius was used for the  $(^3\text{He},d)$  reaction.

indicate that the probabilities of transitions leading to the positive-parity first and second excited states in  $^{15}\text{O}$  and  $^{15}\text{N}$  are much smaller than those for the  $p$ -hole states. Thus, the transitions leading to the 0 and 6.16-MeV states in  $^{15}\text{O}$  should constitute most of the observed integral cross section, if the reaction proceeds by a direct interaction.

With these two  $p$  states assumed to be the sole contributors to the  $^{16}\text{O}(^3\text{He},\alpha)^{15}\text{O}$  reaction, we calculated the integral excitation function with the DW theory. The input optical-model parameters of Alford *et al.*<sup>14</sup> that were used are shown in Table III; these parameters are defined in Ref. 21. The spectroscopic factor required in Eq. (2) is, in the case of pickup from a closed shell, simply the number of equivalent neutrons available in that shell. For the pick-up of  $p_{1/2}$  and  $p_{3/2}$  neutrons from  $^{16}\text{O}$ , the spectroscopic factors are 2 and 4, respectively. The comparison of the experimental and calculated curves is presented in Fig. 8, where the solid curve is that calculated with the parameters in Table III; the dashed curves represent the 21% uncertainty in the empirical normalization factor<sup>14</sup> of 24 that we used. It should be noted that we have assumed that the parameters determined at 8 MeV by Alford *et al.* are applicable at all energies. Actually, they found a small energy dependence between 8 and 10 MeV in the real and imaginary parts of their optical-model potentials. The dotted curve in Fig. 8 shows the variation in cross section calculated with their energy-dependent potentials; the agreement with our experimental points at 7.8 and 8.9 MeV is excellent. Unfortunately, attempts at extrapolating the potentials down to 3 MeV led to an unrealistic excitation function that satisfactorily followed our data points from 8.9 to  $\sim 6$  MeV, but then rapidly increased in magnitude. The calculation with constant potentials is seen in Fig. 8 also to agree with our data points above 7 MeV. Below this energy, the calculation underestimates the magnitude of the cross section, an effect that may be caused by the assumption of energy-independent potentials. Another possible explanation for this property of the calculation is that the empirical normalization factor of Alford *et al.* may be energy dependent. For example, the normalization factor determined for the  $^{13}\text{C}(^3\text{He},\alpha)^{12}\text{C}$  reaction was

found to increase with decreasing energy.<sup>36</sup> However, it may be that this discrepancy between theory and experiment is correct, for Hinds and Middleton<sup>11</sup> observed a resonance in the  $^{15}\text{O}$  ground-state excitation function at 5.8 MeV. They concluded that the  $^{16}\text{O}(^3\text{He},\alpha)^{15}\text{O}$  reaction proceeds predominantly via a direct process at 9 MeV, but that at energies of  $\sim 6$  MeV and below, compound-nucleus formation may still be important.

#### The $^{19}\text{F}(^3\text{He},\alpha)^{18}\text{F}$ Reaction

The optical-model parameters for the entrance  $^3\text{He}+^{19}\text{F}$  channel at 10 MeV have recently been determined by Siemssen *et al.*<sup>15</sup> Because their values differ only slightly from those used for  $^3\text{He}+^{16}\text{O}$ , and because no parameters are presently available for the exit channel,  $\alpha+^{18}\text{F}$ , we have used the same parameters for the  $^{19}\text{F}(^3\text{He},\alpha)^{18}\text{F}$  reaction as for the  $^{16}\text{O}(^3\text{He},\alpha)^{15}\text{O}$  computation. The normalization factor of 24 was also assumed to be applicable to the reaction on  $^{19}\text{F}$ . Although the separation energy of the least-bound particle in  $^{18}\text{F}$  is 4.4 MeV, only states<sup>25</sup> up to 1.7 MeV were considered in our calculations because neither

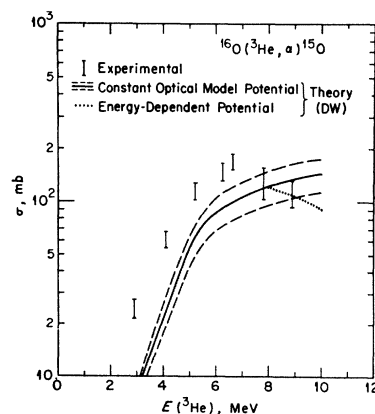


FIG. 8. The  $^{16}\text{O}(^3\text{He},\alpha)^{15}\text{O}$  reaction. Comparison of the experimental excitation function with the results of the DW theory, in which only transitions to the ground and 6.16-MeV states of  $^{15}\text{O}$  were considered significant. See Refs. 13 and 14.

<sup>36</sup> E. M. Kellogg (private communication).



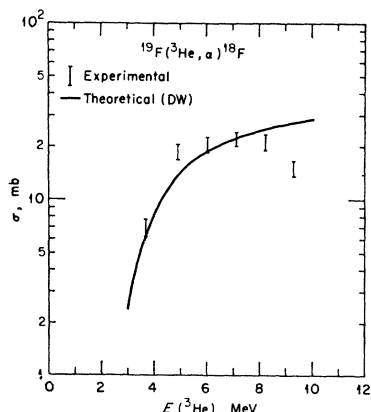


FIG. 9. The  $^{19}\text{F}(^3\text{He}, \alpha)^{18}\text{F}$  reaction. Comparison of the experimental excitation function with the results of the DW theory, in which transitions to only the 0, 0.94, 1.0–1.1, and 1.7 MeV states of  $^{18}\text{F}$  were treated.

spin values nor spectroscopic factors have been determined for the higher-energy states. The energies of the  $^{18}\text{F}$  states, in MeV, treated in the DW calculation and the angular momenta, written in parentheses, of the neutrons transferred in the transitions leading to each state were, respectively, 0 ( $l=0$ ), 0.94 ( $l=2$ ), 1.0–1.1 ( $l=0$ ), and 1.7 ( $l=0$ ); corresponding spectroscopic factors, obtained from the  $^{19}\text{F}(p, d)^{18}\text{F}$  reaction,<sup>28</sup> were 0.6, 0.7, 0.6, and 0.1. Figure 9 presents a comparison of the results of the calculation with our data. The excellent agreement observed depends in detail upon the values that were assumed for the optical-model potentials. Nevertheless, the calculation is significant because a change in optical-model parameters should not drastically affect the shape of the theoretical curve. It should be stressed that the DW calculations appear to explain the large difference, of a factor of  $\sim 5$ , between the cross sections for the  $(^3\text{He}, \alpha)$  reactions on  $^{16}\text{O}$  and  $^{19}\text{F}$ . Neither the differences in  $Q$  values nor  $l$  dependence for these pickup reactions seem to be too important; the reduced cross sections from the JULIE code are not very different for the  $^{16}\text{O}$  and  $^{19}\text{F}$  reactions. But the spectroscopic factors for the  $^{15}\text{O}$  states of importance are 2 and 4, while, for the  $^{18}\text{F}$  states, they have values of 0.7 or less. Thus, the detailed differences in nuclear structure between  $^{16}\text{O}$  and  $^{19}\text{F}$  that are reflected in the very different spectroscopic factors for these nuclides account for the smaller  $^{18}\text{F}$  cross sections that were observed.

#### The $^{12}\text{C}(^3\text{He}, \alpha)^{11}\text{C}$ Reaction

Hinds and Middleton<sup>8</sup> and Alford *et al.*<sup>37</sup> have investigated this reaction in differential experiments above  $\sim 6$  MeV. Their results are in general agreement; the differential excitation function for the transition to the ground state of  $^{11}\text{C}$  exhibits a large resonance at  $\sim 9$

MeV, as well as smaller peaks at lower energies. The angular distributions are also affected by the resonance at  $\sim 9$  MeV, for the magnitude of the forward peak varies by a factor of  $\sim 3$  over the energy interval from 8.5 to 10 MeV. However, the angular distribution still has the shape characteristic of a direct pickup reaction. These results indicate that compound-nucleus processes are effectively competing with a direct-interaction mechanism in this reaction.

To see what the DW theory would predict for the pickup part of the  $^{12}\text{C}(^3\text{He}, \alpha)^{11}\text{C}$  reaction, we computed the integral excitation function using the parameters of Alford *et al.*<sup>35</sup> shown in Table III and a normalization factor of 24. Only the  $l=1$  transition to the  $p_{3/2}$  ground state of  $^{11}\text{C}$  was assumed to be important in the reaction; the  $^{12}\text{C}$  ground state was taken to be a closed  $p_{3/2}$  shell, so that a spectroscopic factor of 4 was used. These assumptions are not unreasonable, because the  $(^3\text{He}, \alpha)$  data of Hinds and Middleton<sup>8</sup> and the  $^{12}\text{C}(p, d)^{11}\text{C}$  experiments of Goodman *et al.*<sup>38</sup> indicate that the total transitions to excited states of  $^{11}\text{C}$  are  $\sim 20\%$  as probable as those to the  $^{11}\text{C}$  ground state. As seen in Fig. 10, the DW contribution to the reaction is a factor of 3 to 4 smaller than the experimental excitation function. This result is consistent with the interpretation, previously discussed, that a significant part of the reaction proceeds through a compound-nucleus mechanism.

#### The $^{12}\text{C}(^3\text{He}, d)^{12}\text{N}$ Reaction

This reaction has been studied by Hinds and Middleton,<sup>8</sup> who found that  $l=1$  stripping best fitted the data

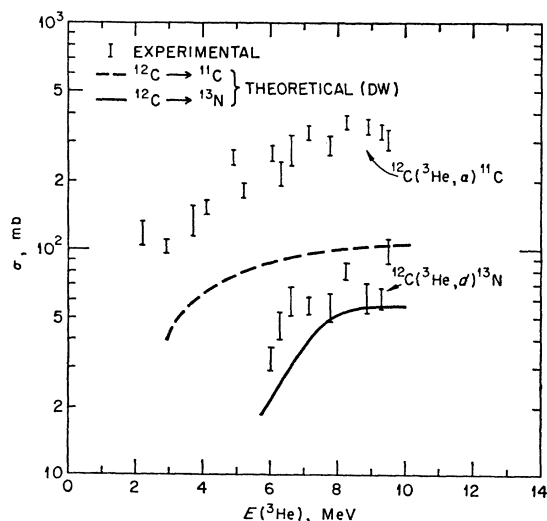


FIG. 10. Comparison of the results of the DW theory for pickup and for stripping reactions with the experimental excitation functions for the  $^{12}\text{C}(^3\text{He}, \alpha)^{11}\text{C}$  and  $^{12}\text{C}(^3\text{He}, d)^{12}\text{N}$  reactions, respectively. In the calculations, only the transitions to the ground states of  $^{11}\text{C}$  and  $^{12}\text{N}$  were considered.

<sup>37</sup> W. P. Alford, L. Blau, D. Cline, and J. Schwartz (to be published).

<sup>38</sup> C. D. Goodman, C. A. Ludemann, and W. H. Kelly (to be published).

for the transition from  $^{12}\text{C}(J=0^+)$  to the  $\frac{1}{2}^-$  ground state of  $^{13}\text{N}$ . Because all of the states above the ground state of  $^{13}\text{N}$  are unstable to particle emission, our integral excitation function was calculated for the ground-state transition only; the calculated curve thus is directly comparable with the differential data of Hinds and Middleton. In our calculations, a spectroscopic factor of 0.7, obtained for the  $^{12}\text{C}(d,n)^{13}\text{N}$  reaction,<sup>28</sup> was used. The overlap factor  $N$  had a value<sup>32</sup> of 8.8. Because the wave function of the deuteron has been extensively studied, we expect that the overlap between  $^3\text{He}$  and  $d+p$  is correctly treated in the DW calculation. Indeed, detailed comparison of our calculated angular distributions with the data of Hinds and Middleton indicate that a normalization factor of only  $\sim 1.5$  is required. Using this value in the computation, and the optical-model parameters of Table III, we obtained from Eq. (3) the calculated integral excitation function that is compared with our results in Fig. 10. The agreement is quite reasonable, indicating that the reaction  $^{12}\text{C} \rightarrow ^{13}\text{N}$  proceeds primarily, if not completely, via the  $(^3\text{He},d)$  stripping mode.

#### V. SUMMARY

A detailed comparison of data from differential and integral experiments for the  $^9\text{Be}(^3\text{He},n)^{11}\text{C}$  reaction showed that the results obtained from the two types of measurements were in agreement.

The distorted-wave theory of direct reactions was used to calculate integral excitation functions for comparison with our data. Optical-model parameters used in the calculations were in all cases taken from differential nuclear-reaction studies, and were not allowed to vary in fitting our data. Only the transitions considered most significant were treated in the computa-

tions. For the  $^{16}\text{O}(^3\text{He},\alpha)^{15}\text{O}$  reaction, only the two negative-parity states in  $^{15}\text{O}$  at 0 and 6.16 MeV, arising from  $l=1$  pickup from closed-shell  $^{16}\text{O}$ , were treated; reactions leading to the positive-parity  $^{15}\text{O}$  states were neglected. In the  $^{19}\text{F}(^3\text{He},\alpha)^{18}\text{F}$  reaction, the states above 1.7 MeV in  $^{18}\text{F}$  were not considered because their spins and parities have not been determined. Only the transition to the ground state of  $^{11}\text{C}$  was calculated for the  $^{12}\text{C}(^3\text{He},\alpha)^{11}\text{C}$  reaction; from other studies, it appears that the sum of the transition probabilities for the excited states of  $^{11}\text{C}$  is  $\sim 20\%$  of that for the ground state. And, since all the excited states in  $^{13}\text{N}$  are unstable to particle emission, only the ground-state transition in the  $^{12}\text{C}(^3\text{He},d)^{13}\text{N}$  reaction was considered.

The agreement between the theoretical and experimental excitation functions was quite reasonable for all the reactions studied save the  $^{12}\text{C}(^3\text{He},\alpha)^{11}\text{C}$  reaction, for which compound-nucleus reactions appear to be predominant. Thus, we conclude that the  $(^3\text{He},\alpha)$  and  $(^3\text{He},d)$  reactions studied in the integral experiments may, in general, be satisfactorily interpreted in terms of direct-reaction mechanisms.

#### ACKNOWLEDGMENTS

We are indebted to G. R. Satchler and R. H. Bassel for their interest in this work, and for many enlightening discussions with them about the distorted-wave theory. The kindness of W. P. Alford, E. M. Kellogg, and C. D. Goodman in making their respective results available to us before publication is appreciated. Thanks are due to J. E. Strain and F. F. Dyer for their help in performing the experiments. Finally, the cooperation of the operating crew of the ORNL 5.5-MeV Van de Graaff accelerator is acknowledged.